

Composition and emission characterization and computational simulation of silicon rich oxide films obtained by LPCVD

M. Aceves-Mijares,^{a*} N. D. Espinosa-Torres,^b F. Flores-Gracia,^b
A. A. González-Fernández,^c R. López-Estopier,^d S. Román-López,^a
G. Pedraza,^a C. Domínguez,^c A. Morales^e and C. Falcony^f

Silicon rich oxide (SRO) is a silicon compatible material that could solve the light emission limitation inherent to bulk silicon. However, not many applications are yet reported, since still much research has to be done. In this paper, SRO superficial films were obtained by low pressure chemical vapor deposition. Structural and optical characterization was done by X-ray photoelectron spectroscopy and Fourier transform infrared spectroscopy (FTIR) corroborating that after annealing, the SiO and the Si₂O phase clearly increases. Emission of SRO in the range between ultra violet and near-infrared is determined by photo, electro and cathode luminescence. Assuming that emission is due to agglomerates of Si–O compounds, computational simulations of cyclic chains of SiO were done to calculate the FTIR spectra, emission and HOMO-LUMO densities. It was found that emission of molecules with less than 10 silicon atoms is not likely to be present in the annealed films. However, for molecules with more than 13 silicon atoms, the emission extends to the visible and near infrared region. The calculated FTIR agrees with the experimental results. Copyright © 2013 John Wiley & Sons, Ltd.

Keywords: photo; electro and cathode luminescence; SRO films; DFT; moieties

Introduction

Silicon rich oxide (SRO) is a multiphase material composed by elemental Si, SiO₂ and SiO_x with x between 0 and 2. Di Maria and coworkers distinguished between low and high density of elemental silicon (or silicon excess) and observed for the first time emission of light by SRO.^[1] This overcoming of the limitations of Si to emit photons has been subject of significant research ever since, in particular, much effort has been devoted to the search for applications of this phenomena. Nevertheless, there is not a clear understanding of the emission mechanisms; many difficulties have been encountered in this enterprise.

The SRO can be obtained by different methods, commonly low pressure chemical vapor deposition (LPCVD) is used because is a simple method that easily allows the fluctuation of silicon excess. In this technique, the partial pressure ratio caused by the flow of reactive gases $Ro = P(N_2O)/P(SiH_4)$ is used to determine the silicon excess. $Ro = 3$ produces a silicon excess of 17 at. %, and $Ro = 100$ is used to obtain stoichiometric silicon dioxide.^[2]

It has been proposed in different paper^[3–5] that in LPCVD SRO the highest light emission has been observed in films with silicon excess in the order of 5 at. % (low silicon excess), which does not contain silicon nano-crystals, but rather silicon oxide defects related to silicon oxidation states. Therefore, in low silicon excess, the emission characteristics should be related to silicon oxidation states, probably amorphous nano-agglomerates (Si nano-points)

The physical microscopic structure of SiO_x is still a subject of discussion, and its arrangement is very important to understand the emission mechanism. A few models are commonly used to describe a SiO_x network: the Mixture Model (MM) by Bell and

Ley,^[6] the Random Bonding Model (RBM) by Philipp^[7] and the Intermediate Model (IM) introduced recently by Novikov and Gritsenko.^[8] The MM approaches to the SiO_x structure as a mixture of two different phases, one of which is richer in oxygen than the other. The RBM describes the SiO_x as a single-phase structure consisting of a number of homogeneously distributed randomly bonded Si-(Si_nO_{4-n}) tetrahedron with n=0, 1, 2, 3, 4. In this case, there should not be any significant variations in the number of oxygen atoms in the vicinity of any given silicon atom, so the oxygen content determined by the position of the Si–O stretching mode should be equal to the macroscopic oxygen content. Finally, IM assumes a smooth variation of the chemical composition at the boundaries between silicon clusters and the SiO₂ matrix, leading to a continuous distribution of the oxygen content.

* Correspondence to: M. Aceves-Mijares, Department of Electronics, INAOE, Puebla, México. E-mail: maceves@ieee.org

a Department of Electronics, INAOE, Puebla, Mexico

b Centro de Investigaciones en Dispositivos Semiconductores, BUAP, Puebla, México

c Department of Micro and Nano Systems, IMB-CNM (CSIC), Spain

d Instituto de Investigación en Comunicación Óptica (IICO), Universidad Autónoma de San Luis Potosí, México

e Centro de Investigación en Materiales Avanzados S. C. Unidad Monterrey-PIIT, México

f Department of Physic, CINVESTAV-IPN, México

The actual structure seems to be greatly determined by the fabrication technique. For example, SiO_x films obtained by magneto-sputtering, plasma-enhanced chemical vapor deposition, and a number of commercially available bulk silicon monoxides have been allocated to the MM whereas the structures of SiO_x films obtained by radio-frequency sputtering and physical evaporation were claimed to match to the RBM.^[9–11] The IM was used by Novikov and Gritsenko^[8] to describe SRO films prepared by LPCVD from a SiH₄ and N₂O source at 750 °C. However, our group also has been modeling the SRO-LPCVD with the RBM^[5].

In this paper, we assume that the emission of SRO obtained by LPCVD is due to SiO agglomerates, especially in the low silicon excess films. SRO films were obtained by LPCVD, and their structural characteristics were studied to corroborate the existence of Si–O bonds. Fourier transform infrared spectroscopy (FTIR), X-ray photoelectron spectroscopy (XPS) and the RBM were used to determine the Si–O compounds in the SRO films. Also, the PL, CL and EL (photo, cathode and electro-luminescence, respectively) of the films were obtained in order to identify the emission range of the films with different silicon excess. Finally, the characteristics of the (SiO) agglomerates were computationally simulated in order to obtain their absorption and emission characteristics and contrast them with experimental FTIR and emission. It was found that some agglomerates with more than 13 Si atoms could emit in the visible to NIR range as SRO does.

Experimental

All SRO films were obtained by LPCVD in a hot wall reactor at around 700 °C, and their partial pressures reactive gases ratios Ro were of 10, 20 and 30 (SRO10, SRO20 and SRO30), corresponding to respective approximated silicon excess of 12, 7 and 5%. After deposition the samples were annealed at 1100 °C in nitrogen gas during 180 min. Light emitting capacitors (LECs) were fabricated in order to obtain the electroluminescence characteristics of the material.^[12] The devices were obtained depositing a 300 nm-thick layer of highly phosphorous-doped polycrystalline silicon on top of approximate 65 nm thick SRO30 films previously deposited on n-type Si wafers with orientation (100) and resistivity between 2 and 5 Ohm-cm. The active layers received the thermal treatment prior to the polysilicon deposition. To fabricate semi-transparent gates, the polysilicon was selectively etched using standard lithography processes in order to define square-shaped contacts with 2 × 2 mm² area. A back contact on the wafers was obtained by the sputtering of around 1.0 μm of Al, and the samples were submitted to standard forming gas procedures to assure ohmic characteristics in the reverse contact.

All measurements were performed at room temperature. The PL spectra were obtained using a HORIBA Jobin Yvon spectrofluorometer model Fluoromax-3, stimulating the SRO samples with 270 nm light and detecting its emission from 400 to 900 nm. The same spectrofluorometer was connected to an optical fiber to perform EL studies to the LECs using only the light detection mode and electrically stimulating the devices between gate and back contact instead of optically. The voltage was applied placing a probe connected to a Keithley 2400 source-meter directly on one corner of the polysilicon gates, and the chuck in which the wafer was placed served as the ground contact. The terminal of the optical fiber from the spectrofluorometer was placed on top and normal to the surface of the gate while applying voltage and measuring current.

Cathode luminescence measurements were performed with a Luminoscope equipment model ELM2-144 at a 0.3 mA current and using energies of 2.5, 5.0, 10.0 and 15.0 keV. The IR spectra were measured with a Bruker FTIR spectrometer model V22, which works in a range of 4000–350 cm⁻¹ with 5 cm⁻¹ resolution. The silicon excess in SRO films was measured with a PHI ESCA-5500 (XPS) using a monochromatic Al radiation source with energy of 1486 eV.

Results and discussion

Structural analysis

Silicon excess in SRO was measured by XPS and an average of 5, 7 and 12 % silicon excess was obtained for SRO 30, 20 and 10, respectively. The microstructure of SRO films was studied analyzing the Si 2p spectra, according with RBM.^[7,13] The Si 2p XPS peaks were decomposed considering the five possible oxidation states for the silicon: Si, Si₂O, SiO, Si₂O₃ and SiO₂. Each oxidation state was fitted using Gaussian distributions, and the energy positions of the different peaks were centered with those previously reported in the literature at approximately 99.8, 100.5, 101.5, 102.5 and 103.5 eV.^[14,15] The relative concentration of each oxidation state was determined and is presented in Table 1; however, specifically in SRO20 and SRO30, the SiO and Si₂O phases clearly increases after annealing.

The SRO films show characteristic infrared absorption peaks associated with the Si–O–Si bonds in SiO₂.^[7,16,17] The FTIR absorbance spectra of SRO samples are depicted in Fig. 1 and were identified as: (1) Si–O rocking at approximately 450 cm⁻¹, (2) Si–O bending at 808 cm⁻¹, (3) Si–H bending at 883 cm⁻¹, (4) Si–O symmetric stretching vibration from 1055 to 1082 cm⁻¹ and (5) Si–O asymmetric stretching at 1170 cm⁻¹.

The as-deposited samples exhibit the characteristic IR absorption due to the stretching vibration of the Si–O–Si bonds about

Table 1. Oxidation states as proposed by the RBM in SRO films with and without annealing at 1100 °C

Oxidation state	Ro = 30	Ro = 30	Ro = 20	Ro = 20	Ro = 10	Ro = 10
	As grown	Annealed	As grown	Annealed	As grown	Annealed
SiO ₂ at %	55.08	47.35	48.28	42.89	48.02	45.86
Si ₂ O ₃ at %	31.60	23.04	34.34	29.39	28.64	19.42
SiO at %	8.18	19.57	9.78	18.23	9.66	13.02
Si ₂ O at %	3.72	7.94	4.96	6.65	9.73	10.53
Elemental Si at %	1.4	2.10	2.64	2.84	3.95	11.18

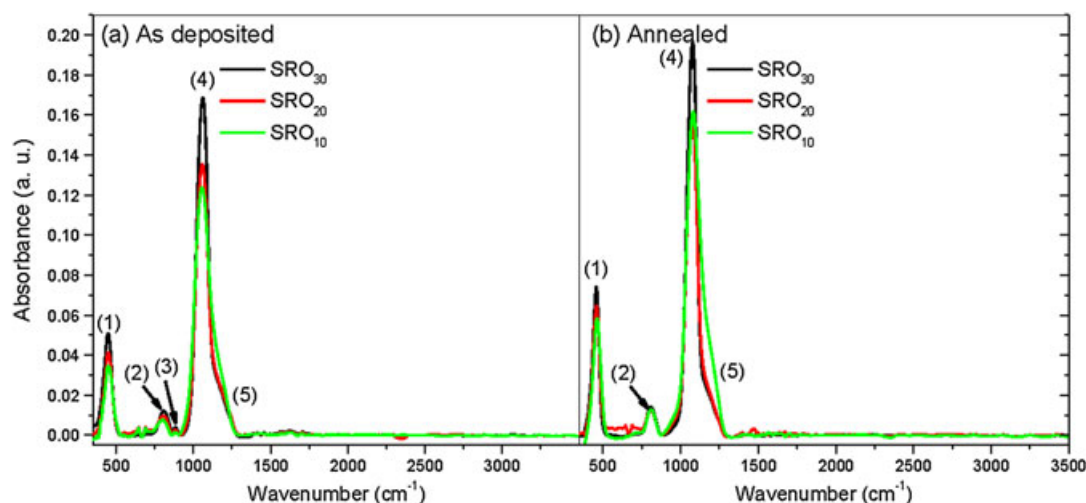


Figure 1. FTIR absorption spectra of SRO films (a) before and (b) after thermal annealing, for the printed black and white publication, the highest peaks 1 and 4 correspond to the SRO30, the medium one is for SRO20 and the smaller one is the SRO10.

1035–1080 cm^{-1} ; the absorbance and frequency of stretching vibration peak decrease as Ro decreases. Figure 1 shows the behavior of the Si–O stretching peak frequency of samples with different silicon excesses. The frequency is lower than that of a SiO_2 film (1080 cm^{-1}) and amorphous a- SiO_2 (1074 cm^{-1}) due to Si atoms replacing O atoms.^[17] Frequency of the Si–O stretching decreases with x of SiO_x . This is related to off-stoichiometric of SRO (silicon excess increases). The stretching frequency increases after annealing for all silicon excess, as shown in Fig. 2; this result suggests an increase of oxidized compounds from the oxide phase and a phase separation during the thermal annealing. The differences between as-deposited and annealed samples could be due to the agglomeration of Si–O bonds, as observed by XPS, specially SiO and Si_2O , which likely can form close (cyclic) and open chains.

Once analyzed by XPS and FTIR the LPCVD-SRO films, there is enough evidence to assume that annealing at 1100 °C produces phase separation of elemental silicon and SiO_x . As can be seen in Table 1, the amount of SiO_x increases as the silicon excess reduces. As the silicon excess moves towards zero, the SRO

becomes SiO_2 . At very high silicon excess, the films evolve towards elemental silicon agglomerates surrounded by SiO_x with $0 < x \leq 2$. In between those extremes, agglomerates of Si–O are likely to form in a matrix of SiO_2 .

Luminescence

The PL, EL and CL-emission spectra of the SRO films are shown in Figs. 3, 4 and 5, respectively. Clearly, the emission of SRO varies in the range of 400 and 850 nm wavelengths. Our group has not observed emission outside of this range, not even with the high excitation energy of cathode electrons.

As can be seen in Fig. 3, photo-luminescence is only observed in annealed samples. As, a matter of fact only samples anneal at 1100 °C produce high emission, and the highest photo emission is obtained for SRO30 films. The PL is only obtained in the visible (VIS) to NIR range, and its intensity reduces as Ro decreases. Comparatively, SRO10 produces negligible emission as that of SRO30.

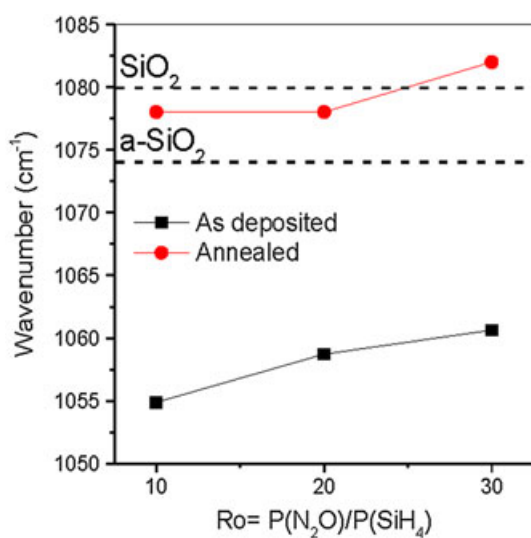


Figure 2. Si–O stretching frequency positions with different Ro, for SRO film before and after annealing at 1100 °C during 180 min.

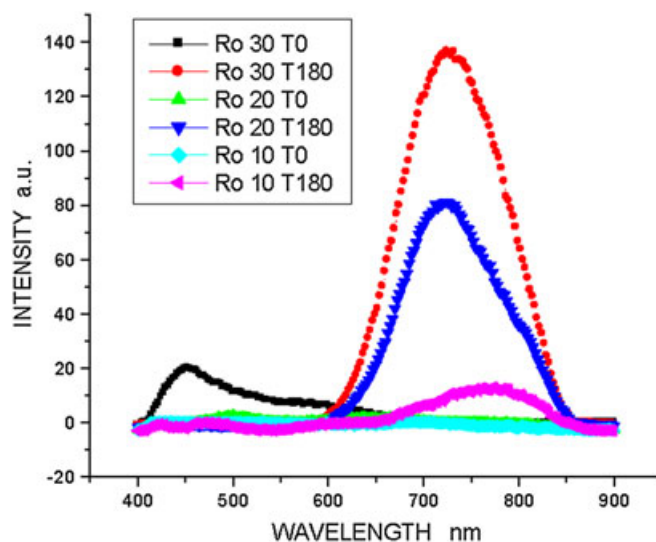


Figure 3. Photo-luminescence for SRO 10, 20 and 30 before and after annealing at 1100 °C for 180 min, for an excitation wavelength of 270 nm.

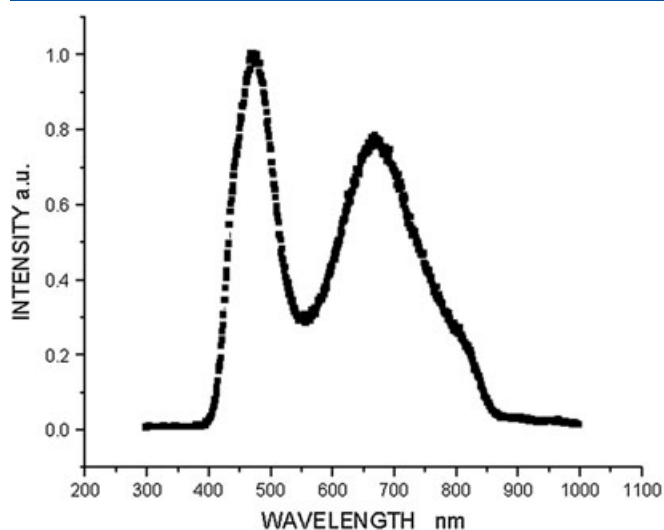


Figure 4. Electro-luminescence of a MOS like capacitor with SRO $R_o = 30$ as dielectric and 50 dc volts applied.

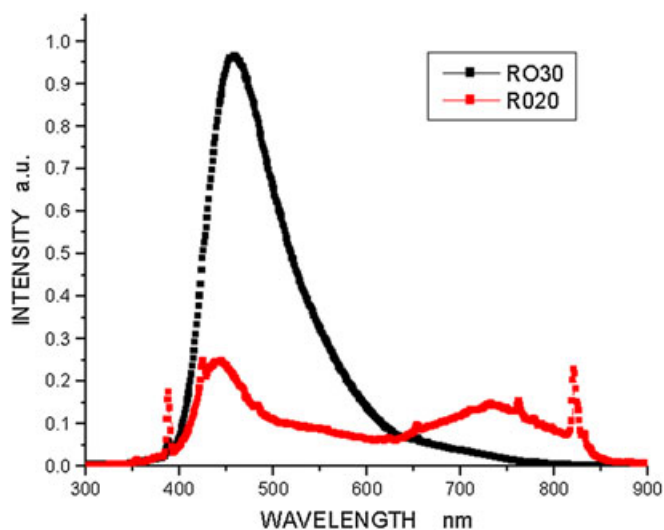


Figure 5. Cathode luminescence at 10 KeV for SRO20 and SRO30 after annealing at 1100 °C during 180 min.

On the other hand, SRO30 cathode luminescence is obtained in the blue side of the spectrum and reduces towards the VIS and NIR region (see Fig. 5). In any case, SRO30 produces the highest emission of the three films. Also, high electroluminescence was observed only in samples with SRO 30, as shown in Fig. 4. In both CL and EL, the blue region is observed indicating that more energetic emission centers can be reached by the high energy excitation electrons.

In reference 4, it is proposed that a competitive mechanism between the high energy electrons and low energy photons is established to reach higher energy centers, and then emit red or blue light.

As mentioned, SRO30 shows PL, EL and CL, and the emission is the more intense of the SRO films. As shown in Table 1, the SRO30 is mainly composed of SiO_x , and it is likely that during annealing, the defects agglomerate forming emission centers. For example, emission at 460 nm, 520 nm and 650 nm

has been attributed to Oxygen Deficiency-related Centers or oxygen vacancies.^[18]

Considering the RBM, Table 1 suggests that agglomerates of any of the oxidation states could be responsible of the SRO emission, particularly for SRO30. Any of the four oxidation states (SiO_2 , Si_2O_3 , SiO and Si_2O) could joint to form agglomerates of two or more molecules. Each set would emit at different wavelength, and summing up all of them, the emission profiles are obtained.

Simulation

As already established, after annealing in the SRO20 and SRO30 films, the SiO and the Si_2O phases percentage increases within the composition of the film, consequently the high emission obtained in films thermally treated is likely related to such oxidation states. The ways in which any of the oxidation states agglomerate or combine with others are endless. Therefore, as a preliminary approach, in this study only, the SiO phase forming cyclic agglomerates with 3 to 21 silicon atoms are computationally simulated. Then, the FTIR and emission properties calculated can be compared with the experimental results. The Si-O simulated arrangements could or not have characteristics like that shown by the SRO, but likely they all are part of the annealed SRO.

Using the program SPARTAN-08^[19] and density functional theory (DFT),^[20–22] with a basis set B3LYP 6-31G*, the IR and UV-Vis spectra for SiO agglomerates were computationally obtained. The simulation of cyclic arrangements with $(\text{SiO})_n$ with $n = 3$ to 21 were done; however, some of them did not converge. Particularly, for FTIR, some other less rigorous methods different than DFT were used to obtain convergence. Then, the simulation results are presented in Tables 2 and 3. In Table 2, the two major FITR calculated peaks are shown as a function of the number of Si atoms for all molecules simulated, and after the table, the main observed peaks are indicated to compare. Also, to compare the major emission peaks are presented in Table 3. Figures 6, 7 and 8 show the spectra of cyclic arrangements with 3, 13 and 20 SiO agglomerates, respectively.

As can be seen in Table 3, the emission for molecules with a reduced number of atoms emit at shortest wavelength, in the UV range. As the number of (SiO) bonds increases, the emission moves towards the visible region of the spectrum.

The orbitals energy, HOMO and LUMO were also calculated, and it was found that they vary with the number of SiO bonds in the molecule. The results are shown in Fig. 9. Clearly, as the number of atoms increases, the band gap reduces, which explains the shift of the emission towards the visible and NIR region of the spectrum. Particularly, when the molecule exceeds 10 silicon atoms, the difference between the highest and the lowest molecular orbitals is reduced abruptly. The inset of Fig. 9 shows the band gap as a function of the number of atoms. We can observe that for 'small molecules' (less than 13 silicon atoms), there is a wide band gap (> 3 eV) whereas for 'large structures' with $n \geq 13$ silicon atoms, the band gap is stretched to approximately 1.6 eV. Hence, it is expected that molecules with 13 silicon atoms or more are responsible for the emission in the visible region of the spectrum, since these molecules present a reduction of the gap energy, and the transition from the orbital HOMO (valence band) to the LUMO orbital (conduction band) is thereby more likely.

Table 2. Calculated frequency vibrations of SiO cyclic structures

Number of silicon atoms	Wavenumber of first peak	Wavenumber of second peak	Number of silicon Atoms	Wavenumber of first peak	Wavenumber of second peak
	cm ⁻¹	cm ⁻¹		cm ⁻¹	cm ⁻¹
3	968	299	13	1055	1046
4	1024	325	14	1070	1047
5	1064	1020	15	1089	1053
6	1008	966	16	N/A	N/A
7	1081	995	17	1029	1022
8	1058	1021	18	1002	978
9	1074	960	19	1022	1013
10	N/A	N/A	20	1032	1003
11	1022	1012	21	1082	1007
12	N/A	N/A			

Experimental Data for FTIR (Ro = 10, 20 and 30) Wavenumber in cm⁻¹ obtained by LPCVD and SiO bending ~808
SiO symmetric stretching 1035–1080 as deposited SiO anti-symmetric ~1170
SiO rocking ~ 450

Table 3. Calculated emission of SiO cyclic structures in UV–Vis-NIR

Number of silicon atoms	Wavelength of first peak more intense	Wavelength of second peak more intense	Wavelength of third peak more intense	Wavelength of fourth peak more intense	Wavelength of fifth peak more intense	Wavelength of sixth peak more intense
	nm	nm	nm	nm	nm	nm
3	293.48					
4	380.33	349.36				
5	321.77	326.41	314.48	288.52	342.55	287.14
6	327.58	312.64	318.42	329.03	328.9	309.95
7	313.86	296.34	300.82	297.53	316.27	298.19
8	346.1	375.31	327.63	335.05	333.47	354.27
9	319.97	319.98	325.69	326.69	326.72	322.53
10						
11	300.09	302.19	315.61	305.05	303.16	321.81
12						
13	914.05	504.62	693.6	573.8	491.66	506.71
14	456.81	462.84	478.8	652.95	490.5	571.33
15	496.48	574.18	534.12	482.54	509.14	615.83
16						
17	496.44	783.22	503.19	1130.05	660.43	583.68
18						
19						
20	477.98	519.93	671.19	595.23	1240.93	543.7
21						

Tables 2 and 3 and Figs. 6, 7 and 8 show the range of absorption and emission of the Si_nO_n cyclic agglomerates obtained computationally, and the comparison with the experimentally obtained can be done. Molecules with only three silicon atoms present anti-symmetrical stretching vibration modes with wavenumbers at 968 cm⁻¹ and at 299 cm⁻¹, and their emission is in the UV range. However, these values are not within the experimentally obtained by FTIR or by any of the luminescence studies. This indicates that these structures are possibly not present in the SRO films.

However, the situation is different for relatively large structures such as (SiO)₁₃ and (SiO)₂₀. As observed in the Figs. 7 and 8, the

calculated stretching vibrational frequencies range goes from 978 to 1055 cm⁻¹. Then, the range and the mode of vibration could be ascribed to molecules contained in the films, agreeing with experimental data. The same argument is valid for the light emission of the mentioned (SiO)₁₃ and (SiO)₂₀. The (SiO)_n agglomerates mentioned as examples are not the only ones, as can be corroborated in the Tables 2 and 3 and Figs. 1–5.

Conclusions

Superficial SRO films with different excess of silicon were obtained by LPCVD, and structural and optical characterizations

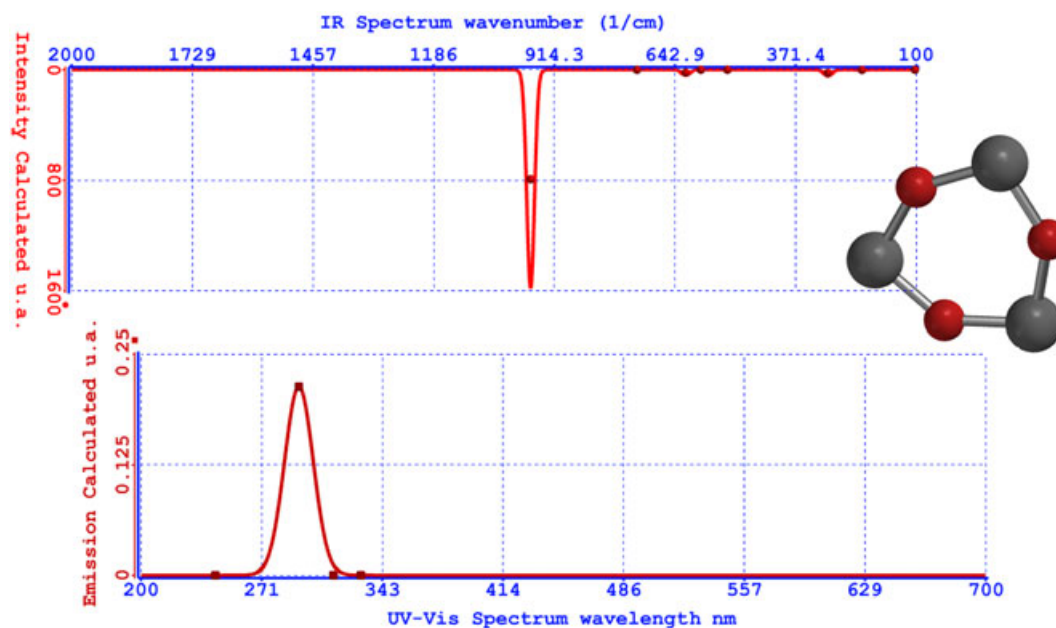


Figure 6. FTIR and emission spectra for a cyclic $(\text{SiO})_3$ agglomerated. A big gray circle represents a silicon atom (radius = 2.1 Å) and a medium red circle is an oxygen atom (radius = 1.52 Å).

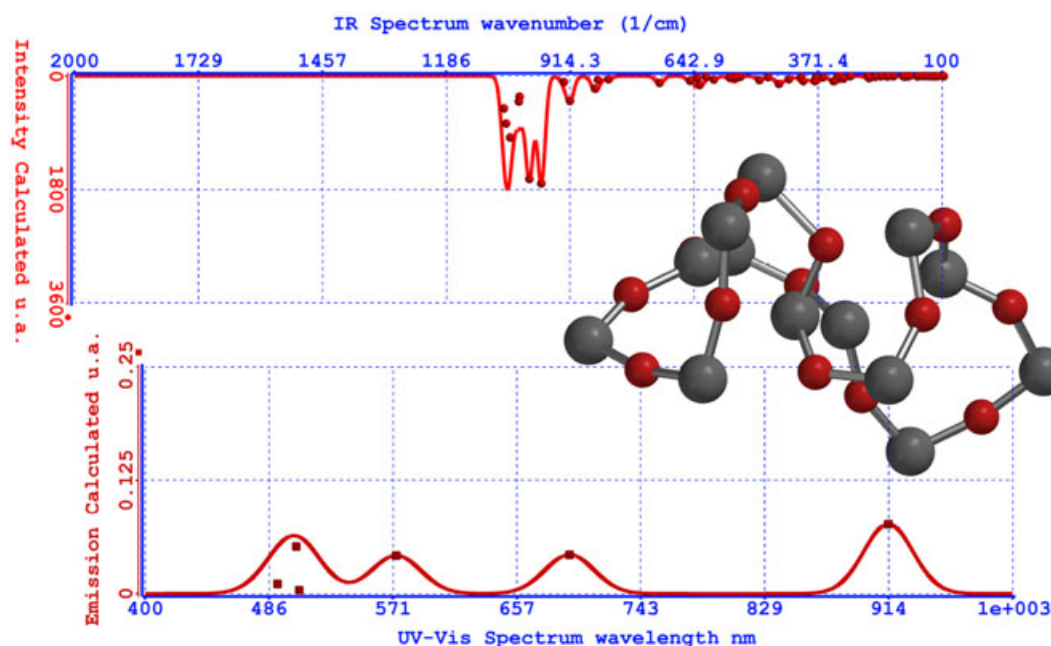


Figure 7. FTIR and emission spectra for a cyclic $(\text{SiO})_{13}$ agglomerated. A big gray circle represents a silicon atom (radius = 2.1 Å), and a medium red circle is an oxygen atom (radius = 1.52 Å).

were obtained. Using XPS, the silicon excess was obtained as a function of the reactive gases ratio R_o with and without annealing. SiO and Si_2O phases clearly increase after thermal treatment. It was also determined that the low silicon excess films have the highest intensity light emission, only after annealing. Then, the SiO and Si_2O agglomerates are likely related to the light emission in SRO annealed obtained by LPCVD. Preliminary, the $(\text{SiO})_n$ agglomerates were

computationally simulated. The range of emission is in the visible to near infrared region of the spectrum. IR absorption and light emission of $(\text{SiO})_n$ molecules was simulated. The simulation results demonstrate that some of these $(\text{SiO})_n$ molecules have absorption and light emission in the range observed in our experimental results, especially molecules with 13, 14, 15 and 20 silicon atoms, indicating that these simulated moieties are part of the annealed SRO-LPCVD films.

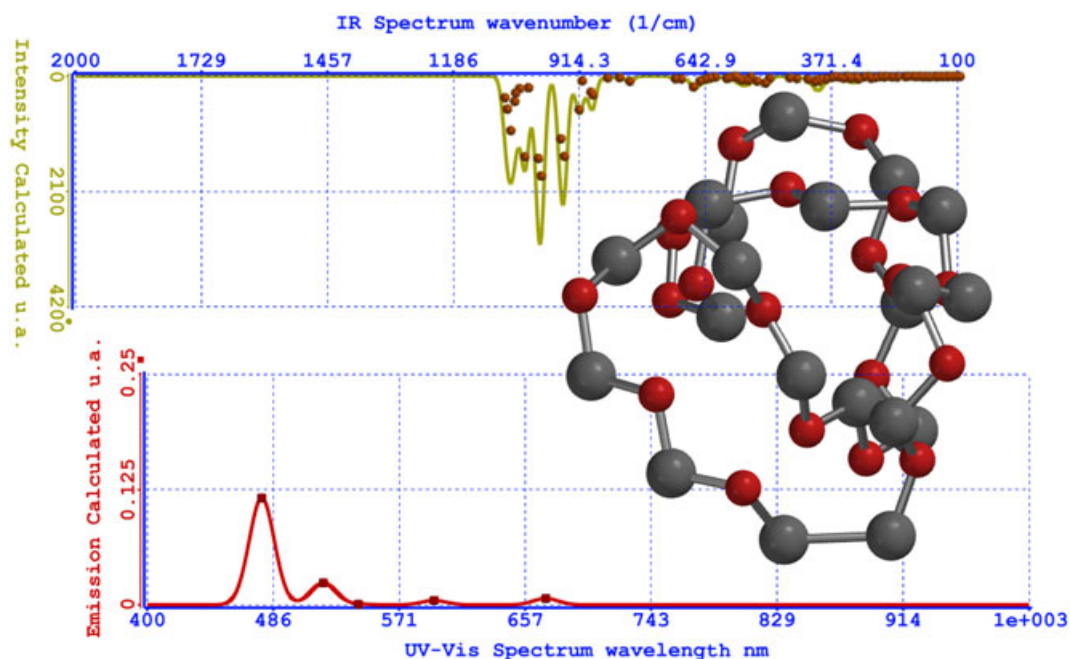


Figure 8. FTIR and emission spectra for a cyclic $(\text{SiO})_{20}$ agglomerated. A big gray circle represents a silicon atom (radius = 2.1 Å), and a medium red circle is an oxygen atom (radius = 1.52 Å).

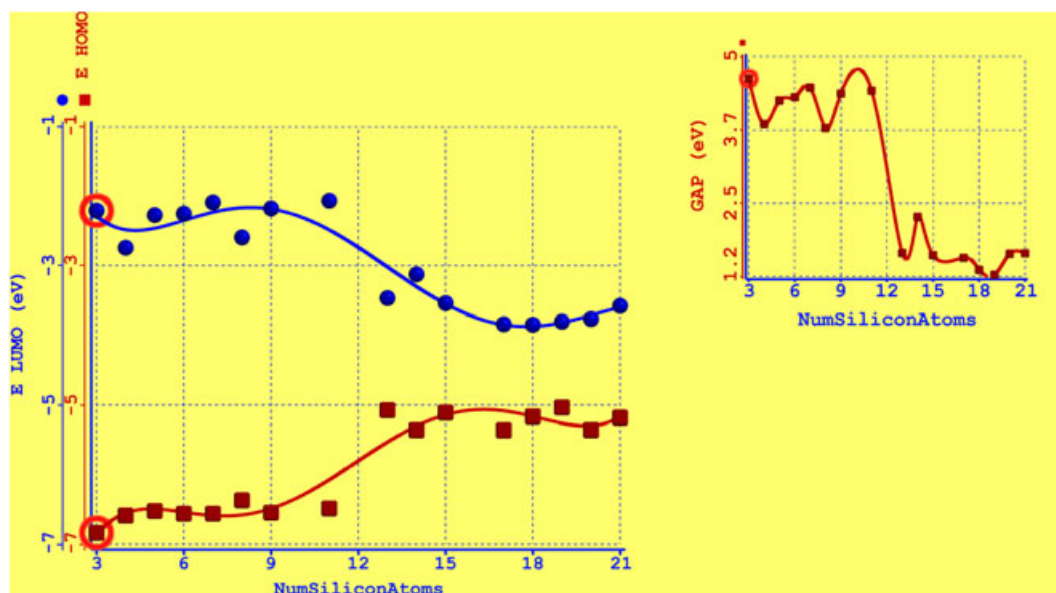


Figure 9. HOMO-LUMO energy density as a function of the number of atoms. The band gap is shown in the inset.

Acknowledgement

The authors appreciate the economic support of CONACYT.

References

- [1] D. J. Di Maria, D. W. Dong, C. Falcony, T. N. Thesis, J. R. Kirtley, J. C. Tsang, D. R. Young, F. L. Pesavento, S. D. Bronson, *J. Appl. Phys.* **1983**, 54(10), 5801.
- [2] D. Dong, E. A. Irene, D. R. Young, *J. Electrochem. Soc.* **1978**, 125(5), 819.
- [3] D. Berman, M. Aceves, A. Gallegos, A. Morales, L. R. Berriel, J. Carrillo, F. Flores, C. Falcony, C. Domínguez, A. Llobera, M. Riera, J. Pedraza, Silicon excess and thermal annealing effects on the photoluminescence of SiO_2 and silicon rich oxide super enriched with silicon implantation. *Phys. Stat. Sol. (C)* **2004**, 1(S1), S83–S87. DOI: 10.1002/pssc.200304864
- [4] M. Aceves-Mijares, A. A. González-Fernández, R. López-Estopier, A. Luna-López, D. Berman-Mendoza, A. Morales, C. Falcony, C. Domínguez, R. Murphy-Arteaga, *J. Nanomater.* **2012**, 2012, Article ID 890701. DOI: 10.1155/2012/890701
- [5] R. López-Estopier, M. Aceves-Mijares, C. Falcony. Cathodo- and Photo- Luminescence of Silicon Rich Oxide Films Obtained by LPCVD, in *Cathodoluminescence* (Ed.: N. Yamamoto), InTech, **2012**, ISBN: 978-953-51-0362-2.
- [6] F. G. Bell, L. Ley, *Phys. Rev. B* **1988**, 37, 8383.
- [7] H. R. Philipp, *J. Phys. Chem. Solids* **1971**, 32(8), 1935–1945.

- [8] Y. N. Novikov, V. A. Gritsenko, *J. Appl. Phys.* **2011**, *110*, 014107.
- [9] A. L. Shabalov, M. S. Feldman, *Thin Solid Films* **1983**, *110*, 215.
- [10] S. M. A. Durrani, M. F. Al-Kuhaili, E. E. Khawaja, *J. Phys. Condens. Matter* **2003**, *15*, 8123.
- [11] A. L. Shabalov, M. S. Feldman, *Thin Solid Films* **1987**, *151*, 317.
- [12] A. A. González Fernández, M. Aceves Mijares, A. Morales Sánchez, K. M. Leyva. Intense whole area electroluminescence from low pressure chemical vapor deposition-silicon-rich oxide based light emitting capacitors, *J. Appl. Phys.* **2010**, *108*, 043105.
- [13] H. R. Philipp, *J. Non-Cryst. Solids* **1972**, *8-10*, 627-632.
- [14] R. Alfonsetti, L. Lozzi, M. Passacantando, P. Picozzi, S. Santucci, *Appl. Surf. Sci.* **1993**, *70-71*(part 1), 222-225.
- [15] D. Q. Yang, J. N. Gillet, M. Meunier, E. Sacher, *J. Appl. Phys.* **2005**, *97*(2), 024303-1-024303-6.
- [16] F. Ay, A. Aydinli, *Opt. Mater.* **2004**, *26*(1), 33-46.
- [17] P. G. Pai, S. S. Chao, Y. Takagi, G. Lucovsky, *J. Vac. Sci. Technol. A: Vac. Surf. Films* **1986**, *4*(3), 689-694.
- [18] M. Cervera, M. J. Hernández, P. Rodríguez, J. Piqueras, M. Avella, M. A. González, *et al.*, *J. Lumin.* **2006**, *117*(1), 95-100.
- [19] W. J. Hehre, *Manual of Software SPARTAN 08. A Guide to Molecular Mechanics and Quantum Chemical Calculations*, Wavefunction, Inc., 18401 Von Karman Ave., Suite 370 Irvine, CA 92612 **2003**.
- [20] R. G. Parr, W. Yang, *Density Functional Theory of Atoms and Molecules*, Oxford University Press, Oxford, **1988**.
- [21] J. K. Labanowski, J. W. Andzelm (Eds), *Density Functional Methods in Chemistry*, Springer-Verlag, New York, **1991**.
- [22] J. M. Seminario, P. Politzer (Eds), *Modern Density Functional Theory: A Tool for Chemistry*, Elsevier, Amsterdam, **1995**.